ACS APPLIED MATERIALS & INTERFACES

Letter

Cite This: ACS Appl. Mater. Interfaces 2018, 10, 39441−39447

www.acsami.org

High-Performance Photocoupler Based on Perovskite Light Emitting Diode and Photodetector

Zhi-Xiang Zhang,[†] Ji-Song Yao,[‡] Lin Liang,[§] Xiao-Wei Tong,[†] Yi Lin,[§] Feng-Xia Liang,*[,§] Hong-Bin Yao,[‡] and Lin-Bao Luo*[,†]

[†]School of Electronic Science and Applied Physics, and Anhui Provincial Key Laboratory of Advanced Materials and Devices, and [§]School of Materials Science and Engineering, Hefei University of Technology, Hefei, Anhui 230009, China

[‡]Hefei National Research Center for Physical Sciences at the Microscale, Department of Chemistry, CAS Center for Excellence in Nanoscience, Hefei Science Center of CAS, University of Science and Technology of China, Hefei, Anhui 230026, China

Supporting Information

ABSTRACT: Photocoupler is a kind of semiconductor optoelectronic device that integrates light-emitting device (LED) and photodetector. It has found wide application in various fields because of its capability to transmit the electrical signal through the conversion of the electricity-light-electricity. Herein, we report the fabrication of a new photocoupler by simply integrating perovskite quantum dots LED and perovskite photodetector on a glass substrate. The as-fabricated photocoupler showed outstanding characteristics with high current transfer ratio (CTR) of 3.35%, which is highly competitive in comparison with other materials based devices. Furthermore, the perovskite photocoupler had a fast response speed of 8 μs/8.26 μs. By further adding an amplification circuit, the CTR could be enhanced by around 50 times to 172.6%. These results indicate that the present perovskite-based photocouplers may find potential application in future integrated circuit and optoelectronic system.

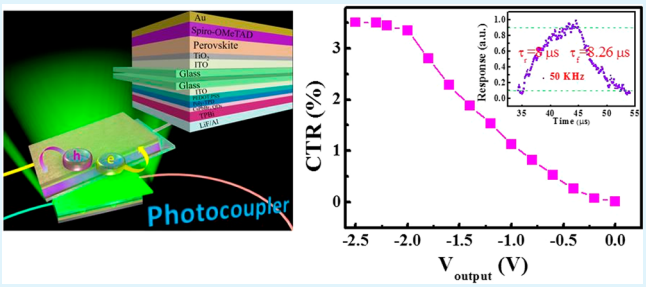

KEYWORDS: *optoelectronic devices, current transmission ratio, perovskite, light-emitting diode, photodetector*

In recent years, perovskite materials with a typical chemical formula of $MPbX_3$ (M = Ma, FA, and Cs, X = Cl, Br, and I) have received enormous research interest because of their larger absorption coefficient, high carrier mobility, tunable band gap, unique crystal structure, low density of defects, and easy processing.[1,2] For example, Kovalenko and co-workers fabricated the cesium lead halides perovskite quantum dots (QDs), which exhibited outstanding optical properties with tunable and high-quantum-yield photoluminescence (PL).[3] By using the $CsPbBr_3$ QDs, Zeng's team successfully fabricated a LED for the first time. The luminance (green light) was as high as 946 cd m^{-2} with an external quantum efficiencies (EQE) of 0.12%.[4] In addition to LEDs, a number of photodetectors with different device configurations including photoconductors, phototransistors and photodiodes have been achieved by using perovskite materials.[5,6] For instance, Yang' team had fabricated a highly sensitive photodetectors based on $CH_3NH_3PbI_{3-X}Cl_X$. The device showed a fast response time of 180/160 ns and high specific detectivity of 4×10^{14} Jones.[7] Moreover, Xie has developed an ultrasensitive photodetector with an ultrahigh EQE of 1.19×10^3% and a responsivity of 3.49 AW^{-1}.[8] Various study have shown that hybrid organic−inorganic perovskite photodiodes usually exhibit inherent advantages in terms of larger specific detectivity, lower noise, and faster response speed over perovskite photoconductors and phototransistors.[9,10]

Photocouplers, as a representative of optoelectronic devices have recently received increasing research interest because of wide application in various fields such as solid state relay, multivibrator, digital gauges, industrial communication and so forth. It is geometrically composed of LED and photodetector, which can transfer electrical signal to optical signal, and finally back to electrical signal.[11−16] To date, a variety of photocouplers have been achieved by using different kinds of materials. Yu et al. in 1994 fabricated a photocoupler using semiconducting polymers, the current transfer ratio (CTR) reached 2×10^{-3}.[12] Yang reported an similar polymer photocoupler which can work at low driving voltage with high current transfer ratios and fast dynamic response.[16] Later, Wang's group reported a photocoupler through integration of a tandem white organic LED light source as input unit and organic/inorganic hybrid heterojunction photodetector as output unit. Device analysis reveals that the CTR was as high as 28.2%. After further amplification, the CTR was increased to 263.3%.[11] Enlightened by the above work, we herein reported a new photocoupler by using $CsPbBr_3$ QDs LED as input unit, and a self-driven $FA_{0.85}Cs_{0.15}PbI_3$ perovskite

Received: September 8, 2018
Accepted: November 6, 2018
Published: November 6, 2018

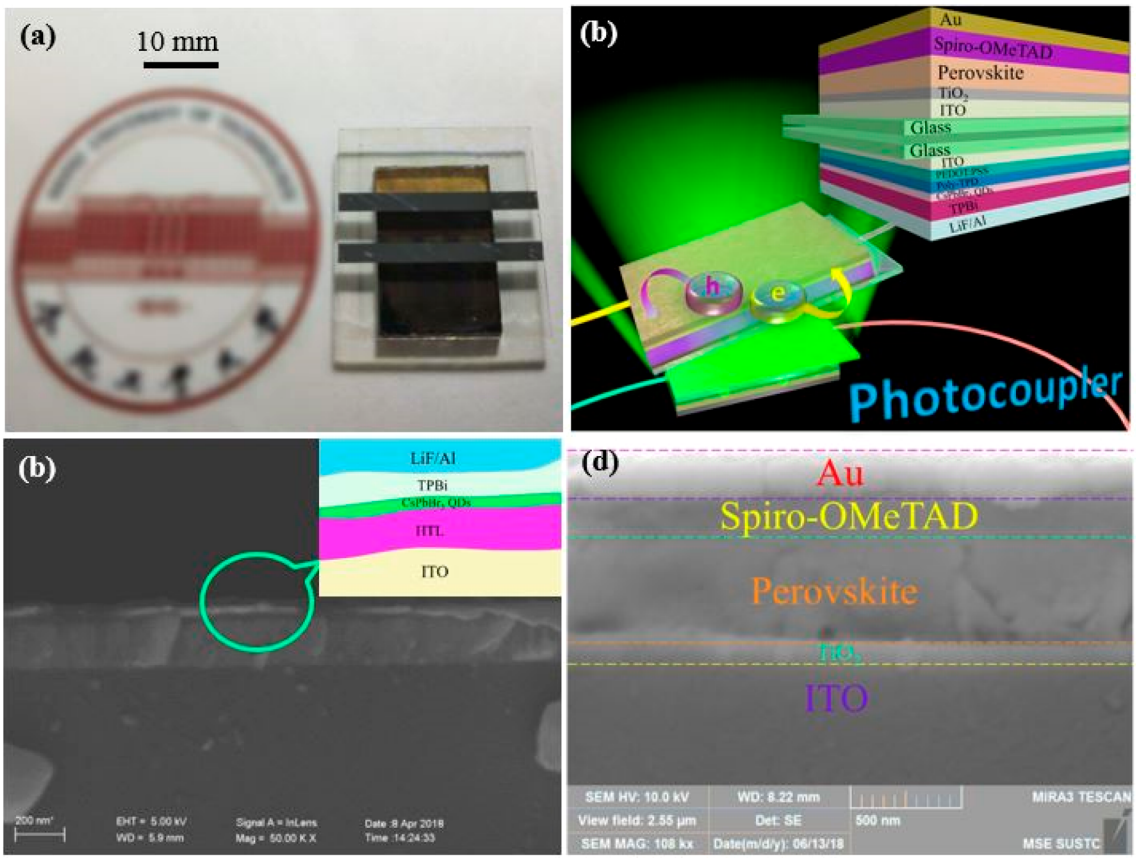

Figure 1. (a) Digital camera picture of the perovskite photocoupler. (b) Schematic illustration of the perovskite photocoupler, the inset shows the device geometries of both perovskite QDs LEDs and perovskite photodetector. (c) Cross-section SEM image of the $CsPbBr_3$ QD LEDs. (d) Cross-section SEM image of the $FA_{0.85}Cs_{0.15}PbI_3$ photodetector.

photodiode as output unit. The $CsPbBr_3$ QDs LED with a structure of indium tin oxide (ITO) glass/PEDOT:PSS/$CsPbBr_3$ QDs/Poly-TPD/TPBi/LiF/Al exhibited high EQE of 1.1%, and the output unit with the structure of indium tin oxide (ITO) glass/TiO_2/$FA_{0.85}Cs_{0.15}PbI_3$/Spiro-OMeTAD/Au exhibited outstanding characteristics in terms of the high detectivity and EQE. The corresponding current transfer ratio (CTR) was estimated to be 3.35%, which is higher than the majority of photocouplers previously reported. By further adding a common-based amplification circuit, the CTR could be increased to 172.6%. More importantly, the present perovskite photocoupler had a fast response speed of τ_r = 8 μs/τ_f = 8.26 μs.

The proof-of-concept photocoupler was composed of perovskite LED and photodetector, both of which are integrated onto a glass substrate (Figure 1a). As illustrated in Figure 1b, the perovskite LED can emit green light that will be further converted into current signal by the perovskite film photodetector. Figure 1c, d shows the cross-section scanning electron microscopy (SEM) images of both LED with a structure of ITO/PEDOT:PSS/$CsPbBr_3$ QDs/Poly-TPD/TPBi/LiF/Al, and photodetector with a structure of ITO/TiO_2/$FA_{0.85}Cs_{0.15}PbI_3$ perovskite/Spiro-OMeTAD/Au, respectively. According to TEM analysis shown in Figure S1, the monodisperse $CsPbBr_3$ QDs obtained from a hot-injection method,[2,17] have a typical cubic shape. The diameter distributes from 5 to 10 nm, with an average value of 8.2 nm (see Figure S1a, b). What is more, from the SEM image shown in Figure S2a, b, the $FA_{0.85}Cs_{0.15}PbI_3$ film used in the photodetector has a relatively continuous surface. The present Cs doped $FAPbI_3$ is similar to the structure of conventional $MAPbI_3$: the FA^+ and Cs^+ cations occupy the eight corner of the cubic unit cell, whereas the Pb atom are located at the central position of a $[PbI_6]^{4-}$ (Figure S2c).[18,19] As a matter of fact, such a structure is further confirmed by XRD pattern in Figure S2d.[20,21]

As revealed by the energy band diagram in Figure 2, the TPBi thin films in the LED are used as electron-transporting layers. In addition, both PEDOT:PSS and Poly-TPD will act as hole transporting layers (HTL). Once applied a bias voltage, the PEDOT:PSS can decrease the hole injection barrier, blocking the electron in the active layer and thereby allowing the holes and electrons to efficiently recombine in the QDs emitting layers.[22] Since the LED is directly in contact with the photodetector, the light emitted from perovskite QDs film is easily absorbed by $FA_{0.85}Cs_{0.15}PbI_3$ thin film. It should be mentioned that the $FA_{0.85}Cs_{0.15}PbI_3$'s highest occupied molecular orbital (HOMO) level is lower than Spiro-OMeTAD's valence band energy level and lowest unoccupied molecular orbital (LUMO) level is higher than TiO_2's conduction band energy level. By this token, the electron−hole pairs could be separated to form the output current of the photocoupler.

During the design of the perovskite photocoupler, the consistency between the emitting spectrum of the $CsPbB_3$ QDs LED and photoresponse spectrum of the $FA_{0.85}Cs_{0.15}PbI_3$ photodetector should be considered in that this factor can greatly influence the device performance. Figure 3a shows the

DOI: 10.1021/acsami.8b15213
ACS Appl. Mater. Interfaces 2018, 10, 39441−39447

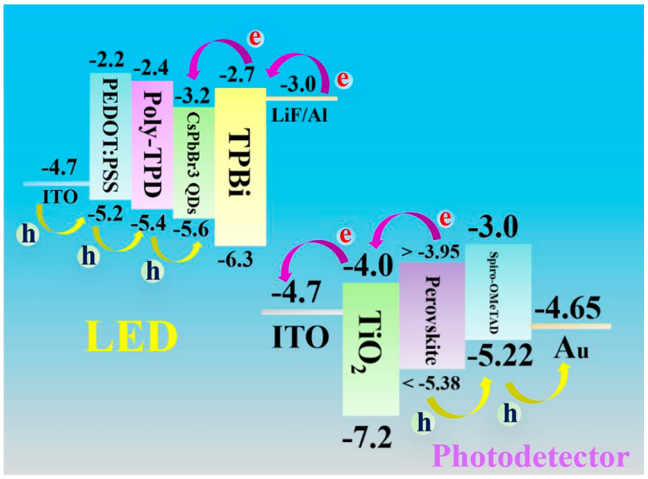

Figure 2. Energy band diagram of perovskite photocoupler composed of $CsPbBr_3$ QDs LED and $FA_{0.85}Cs_{0.15}PbI_3$ photodetector.

normalized electroluminescence (EL) spectrum of the LED device. It is obvious that at applied voltage of 7 V, the device gives a very narrow EL spectrum at 514 nm which is solely attributed to the band-edge emission of QDs. Such an EL characteristic is in consistence with the corresponding photoluminescence (PL) spectrum taken from QDs in colloid solution (Figure S3a).[23,24] Further current density−luminance−voltage (J−L−V) curve in Figure 3b reveals that the LED exhibits a luminance as high as 1713.4 cd m^{-2}, with a maximum current efficiency of 3.24 cd A^{-1} (Figure 3c) and external quantum efficiency (EQE) of 1.11% (Figure S3b). Such values are much better than previous work in which the maximum current efficiency, EQE and luminance were 0.43 cd A^{-1}, 0.12%, and 100 cd m^{-2}, respectively.[4] What is more, the device shows a saturated and pure colors, as demonstrated by the Commission Internationale de l'Eclairage (CIE) color coordinate located at (0.0621,0.7045) (Figure 3d). With regard to the $FA_{0.85}Cs_{0.15}PbI_3$ perovskite photodetector, it is actually a typical photovoltaic photodetector. The reason why we choosing $FA_{0.85}Cs_{0.15}PbI_3$ to fabricate the photodiode photodetector is simply because such structure can offer a relatively high and stable photocurrent, which is very beneficial for CTR. As exhibited in Figure 3c, the ITO/TiO_2/$FA_{0.85}Cs_{0.15}PbI_3$perovskite/Spiro-OMeTAD/Au photodetector

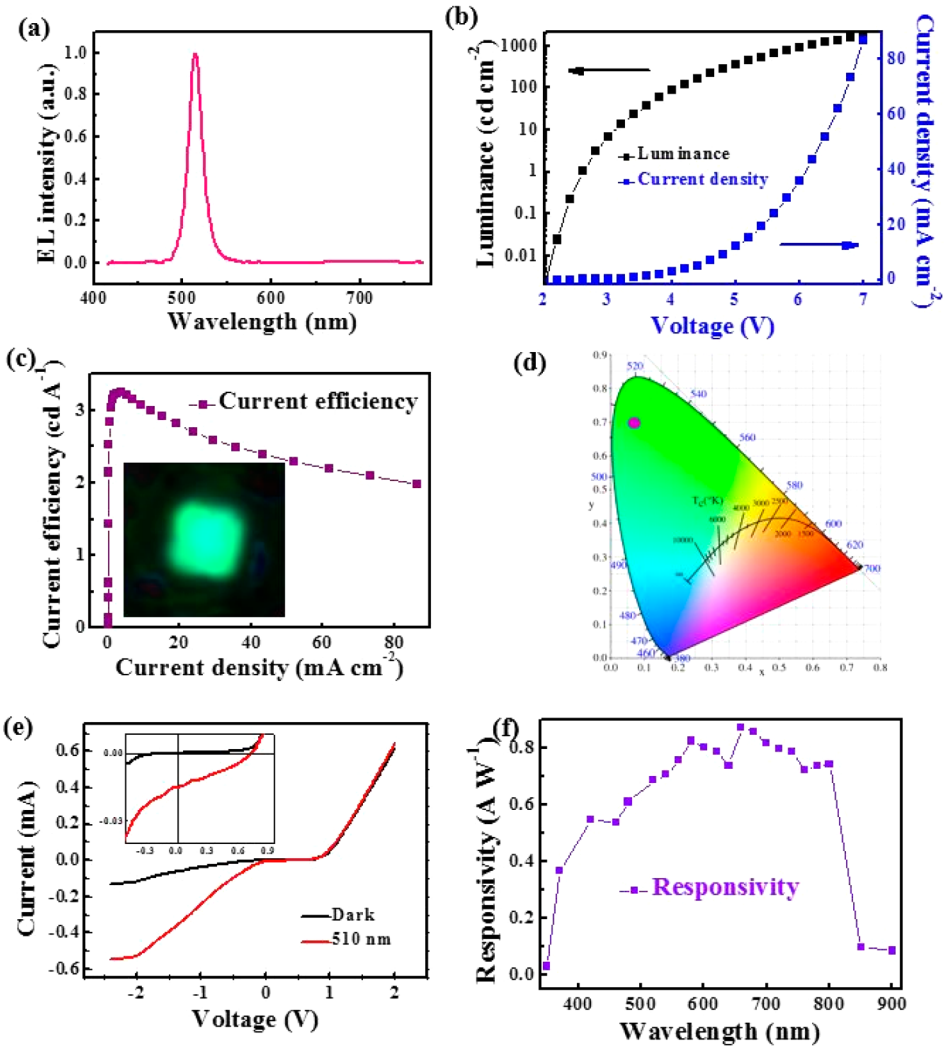

Figure 3. (a) EL spectrum of the $CsPbBr_3$ QDs LED. (b) J−L−V curve of the $CsPbBr_3$ QDs LED. (c) Current efficiency of the $CsPbBr_3$ QDs LED. (d) CIE coordinate of the $CsPbBr_3$ QDs LED. (e) I−V characteristics of the $FA_{0.85}Cs_{0.15}PbI_3$ perovskite photodetector in the dark and illuminated with 510 nm light (0.3 mW cm^{-2}). (f) Wavelength-dependent responsivity of the photodetector.

DOI: 10.1021/acsami.8b15213
ACS Appl. Mater. Interfaces 2018, 10, 39441−39447

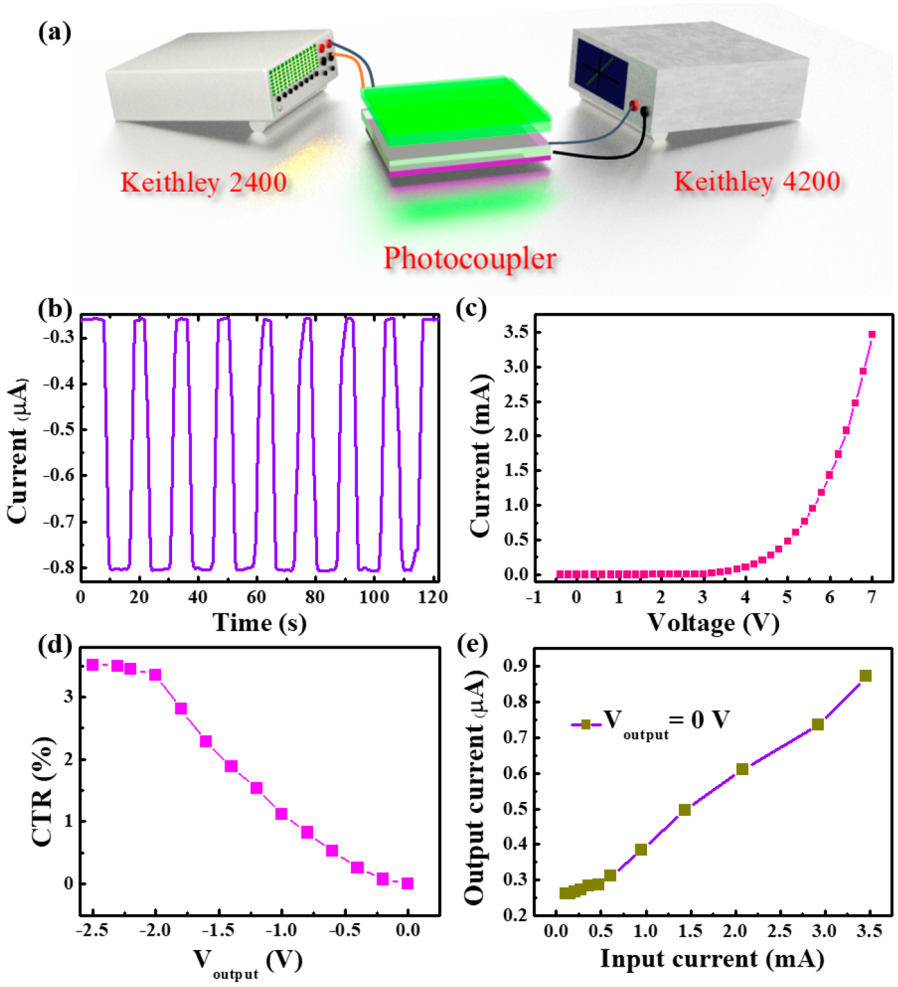

Figure 4. (a) Schematic illustration of the setup for measuring the device performance of the perovskite photocoupler. (b) Time-dependent photoresponse of the coupler. (c) Current−voltage curve of the perovskite LED. (d) CTR of the photocoupler as a function of different V_{output}. (e) I_{out}−I_{in} characteristic of the photocoupler.

shows obvious photovoltaic characteristics once illuminated by 510 nm light, with an open-circuit voltage (V_{OC}) of 0.72 V and a short-circuit current (I_{SC}) of 0.015 mA under 0.3 mW cm^{-2}. Although the corresponding power conversion efficiency is relatively low, it however could provide a high photocurrent at relatively low bias voltage. Without question, this will be good for highly CTR. On the other hand, unlike other perovskite material based photoconductors or phototransistors, this photovoltaic photodetector has very fast response speed, which is highly beneficial for the response speed of perovskite photocoupler. Based on the responsivity (0.7 A W^{-1} at 510 nm), the corresponding specific detectivity (D^*) and EQE were estimated to be 1×10^{12} Jones, 160%, respectively (see Figure S4a, b, the detailed calculation of the R, D^*, and EQE are provided in the Supporting Information).[25]

To examine the device performance of the perovskite photocoupler, we used a Keithley 2400 to drive the LED and Keithley 4200 to study the photodetector (Figure 4a). Figure 4b, c shows the C−V curve of the $CsPbBr_3$ QDs LED and time-dependent photoresponse of the photodetector, respectively, when the LED was applied by a voltage of 7 V and the $FA_{0.85}Cs_{0.15}PbI_3$ photodetector was zero biased. Apparently, the perovskite photocoupler can work properly: The perovskite photodetector can absorb the light emitted from $CsPbBr_3$ QDs LED and generate photocurrent, thus realizing the electricity-light-electricity conversion. To quantitatively evaluate the device performance of this perovskite photocoupler, the CTR that is defined as the ratio of current of photodetector (output unit) to the current of LED (input unit) (CTR = I_{output}/I_{input}),[16] is calculated to be 3.35% (Figure 4d), at an output voltage of −2 V. In fact, the CTR of the present perovskite photocoupler is highly dependent on bias voltage applied on the photodetector. In the region from 0 to −2 V, with the increase of the bias voltage (absolute value), the CTR is observed to increase gradually. Nonetheless, with the further increase in bias voltage, the CTR begin to saturate. Such a saturation in CTR is understandable as the photocurrent of the perovskite photodetector begins to saturate at high reverse bias voltage (Figure 3b). Even though the CTR of our device performance is smaller than the previous organic-perovskite photocoupler,[11] but is much higher than C_{60}/*N*,*N*′-diphenyl-*N*,*N*′-bis(1-naphthyl)(1,10-biphenyl)-4,40-diamine hybrid heterojunction photocoupler,[13] all-organic photocoupler,[14,15] all-polymeric photocoupler,[16] and even the amorphous SiC:H/SiGe:H photocoupler[26](see Table 1). We believe the CTR can be further optimized by composition engineering, or surface passivation, which can substantially the EQE of perovskite LEDs. Moreover, replacing the perovskite LEDs with other $CsPbBr_3$ devices with higher efficiency can also increase the CTR.[27−29] In addition to the relatively large CTR, our

DOI: 10.1021/acsami.8b15213
ACS Appl. Mater. Interfaces 2018, 10, 39441−39447

Table 1. Comparison of the Device Parameters of the Present Photocoupler with Other Photocouplers Reported Previously

photocoupler	τ_r/τ_f	CTR (%)	driving voltage (LED/ photodetector) (V)	ref
all-perovskite photocoupler	8 μs/ 8.26 μs	3.35	7/2	our work
OLED/perovskite photocoupler	17 μs/ 20 μs	28.2	6/3	11
organic photocoupler	1.18 μs/ 0.74 μs	0.17	5/3	13
organic photocoupler		0.6		14
organic photocoupler	6.5s	3×10^{-3}	6/15	15
all-polymeric photocoupler	0.5 μs	1.5	5/0	16
amorphous photocoupler		1×10^{-4}	20/0	26

photocoupler also can work in a wide current range. Figure 4e shows the current transfer characteristic of the photocoupler at V_{output} = 0 V. It can be easily seen that I_{output} increases linearly with I_{input}, suggesting potential application of this perovskite photocoupler in analog circuits.

For practical application, amplification circuits are often incorporated in the photocoupler, in order to boost the CTR value. In this study, via similar approach, we achieved a CTR as high as 172.6%. Figure 5a schematically illustrates the common-base amplification circuit. A low-power negative−positive-negative silicon transistor which is one of the most commonly used semiconductor transistor models in circuit hardware design was employed. One can easily find that the CTR is substantially increased by about 50 times at an applied bias of −2 V, whereas there is no obvious increase in CTR at applied bias of 0 V because of the invalidation of the amplification circuit at zero bias (Figure 5b). Considering the fact that commercial photocouplers usually have CTR values of 50−200%, therefore the present perovskite photocoupler shows promise as an alternative to commercial inorganic photocoupler in the fields such as computer, peripheral interface, high-speed digital systems, artificial machine intelligence, and so on.

Besides CTR, the response speed which reflects the capability of photocoupler to follow a rapidly changing light signal was also examined. Generally speaking, photocouplers with fast response speed are highly favorable as they could greatly expand the application of photocoupler in digital signal processing. Figure 6a displays the emitting images of the LEDs that are recorded at different frequencies of 1 Hz, 5 kHz, and 100 kHz, in which no obvious degradation in luminous intensity was observed. However, with the further increase of the input voltage frequency from 200 to 250 kHz, the brightness of the LED will greatly decrease. Specifically, the perovskite QDs LED will not work any longer when the frequency reaches 300 kHz. Such an evolution in luminous intensity is due to the decreased capacitive reactance at high frequency.[30] From the transient photoresponse of the perovskite photocoupler in Figure 6b−d, our photocoupler displayed excellent switching characteristics and good reproducibility at frequency of 1 Hz, 5 kHz, 50 kHz. According to a single normalized cycle of the photoresponse curve under 50 kHz light illumination shown in Figure 6e, the rise time (τ_r) and fall time (τ_f) which are the duration for the signal to vary from 10 to 90% (rise time), 90 to 10% (fall time),[11] were estimated to be 8 and 8.26 μs, respectively. This response speed is faster than that of OLED/Perovskite photocoupler,[11] and all-organic photocoupler,[15] but is poorer than all-polymeric photocoupler and C_{60}/*N*,*N*′-diphenyl-*N*,*N*′-bis(1-naphthyl)(1,10-biphenyl)-4,40-diamine hybrid heterojunction photocoupler (see Table 1). As a matter of fact, the switching speed can be further optimized by eliminating charge trapping and removing the constraints from the resistance-capacitance constant. Regarding to the pros and cons of this photocoupler, the main advantage is obviously associated with its ease of fabrication. The perovskite materials can be easily synthesized by using solution based method, which is more convenient than the conventional photocouplers (AlGaAs or GaAsP) that usually entail the complicated synthesis using MOCVD. Undeniably, this perovskite photocoupler is not stable because of the poor ambient stability of perovskite material, which constitutes the main disadvantage.

In summary, a high-performance photocoupler based on $CsPbBr_3$ QDs LED and $FA_{0.85}Cs_{0.15}PbI_3$ film photodetector has been fabricated. Thanks to the photovoltaic characteristics of the perovskite photodetector, the as-assembled perovskite photocoupler achieved a CTR of 3.35%, which is much larger than most of other materials based photocouplers. In addition, such a perovskite photocoupler has a fast response (rise time/ fall time: 8 μs/8.26 μs). By employing an amplification circuit, the CTR can be further increased by nearly 50 times to 172.6%, which is close to that of commercial photocoupler. The generality of the above results suggests the great potential

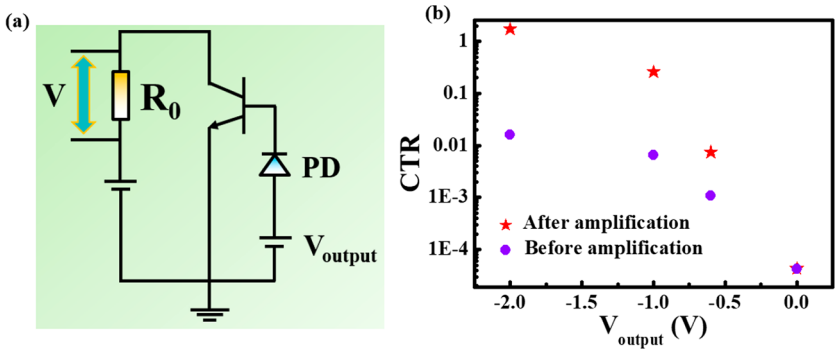

Figure 5. (a) Common-base amplification circuit of the photocoupler in amplified rotational state. (b) CTR of the photocoupler under different applied photodetector bias with and without an amplification circuit.

DOI: 10.1021/acsami.8b15213
ACS Appl. Mater. Interfaces 2018, 10, 39441−39447

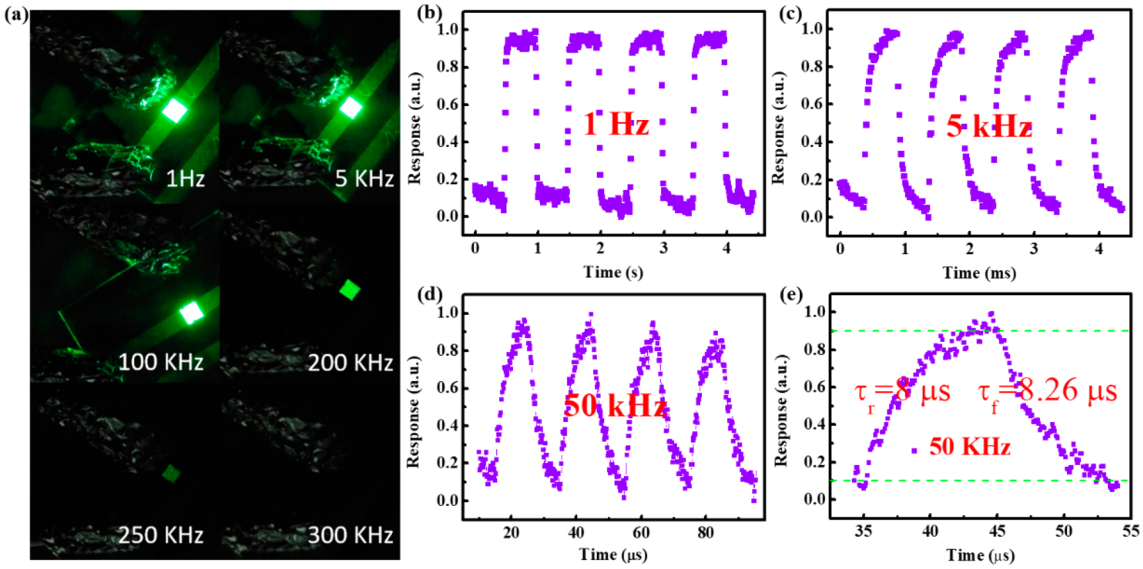

Figure 6. (a) Emitting images of the LED driven by different frequencies at 7 V bias. The photoresponse of the photocoupler with frequency of (b) 1 Hz, (c) 5 kHz, and (d) 50 kHz. (e) Single normalized cycle of the photoresponse for estimating the rise and fall times at the frequency of 50 kHz.

of our perovskite photocoupler in future optoelectronic systems and large-scale integrated circuit application.

■ ASSOCIATED CONTENT

Supporting Information

The Supporting Information is available free of charge on the ACS Publications website at DOI: 10.1021/acsami.8b15213.

Experimental section, TEM images of $CsPbBr_3$ QDs, SEM image of $FA_{0.85}Cs_{0.15}PbI_3$ film, XRD analyses of $FA_{0.85}Cs_{0.15}PbI_3$ film, PL of the $CsPbBr_3$ QDs, EQE of the $CsPbBr_3$ QDs LED, the method for calculating responsivity, specific detectivity, EQE of the perovskite photodetector (PDF)

■ AUTHOR INFORMATION

Corresponding Authors

*E-mail: liangfx@hfut.edu.cn.

*E-mail: luolb@hfut.edu.cn.

ORCID

Hong-Bin Yao: 0000-0002-2901-0160

Lin-Bao Luo: 0000-0001-8651-8764

Notes

The authors declare no competing financial interest.

■ ACKNOWLEDGMENTS

This work was supported by the National Natural Science Foundation of China (NSFC 61675062, 61575059, and 21501038), the Fundamental Research Funds for the Central Universities (JZ2018HGPB0275, JZ2018HGTA0220), and the China Postdoctoral Science Foundation (103471013).

■ REFERENCES

(1) Wang, H.; Kim, D. H. Perovskite-Based Photodetectors: Materials and Devices. *Chem. Soc. Rev.* **2017**, *46* (17), 5204−5236.

(2) Pan, J.; Quan, L. N.; Zhao, Y.; Peng, W.; Murali, B.; Sarmah, S. P.; Yuan, M.; Sinatra, L.; Alyami, N. M.; Liu, J. K.; Yassitepe, E.; Yang, Z. Y.; Voznyy, O.; Comin, R.; Hedhili, M. N.; Mohammed, O. F.; Lu, Z. H.; Kim, D. H.; Sargent, E. H.; Bakr, O. M. Highly Efficient Perovskite-Quantum-Dot Light-Emitting Diodes by Surface Engineering. *Adv. Mater.* **2016**, *28* (39), 8718−8725.

(3) Protesescu, L.; Yakunin, S.; Bodnarchuk, M. I.; Krieg, F.; Caputo, R.; Hendon, C. H.; Yang, R. X.; Walsh, A.; Kovalenko, M. V. Nanocrystals of Cesium Lead Halide Perovskites ($CsPbX_3$, X = Cl, Br, and I): Novel Optoelectronic Materials Showing Bright Emission with Wide Color Gamut. *Nano Lett.* **2015**, *15* (6), 3692−3696.

(4) Song, J.; Li, J.; Li, X.; Xu, L.; Dong, Y.; Zeng, H. B. Quantum Dot Light-Emitting Diodes Based on Inorganic Perovskite Cesium Lead Halides ($CsPbX_3$). *Adv. Mater.* **2015**, *27* (44), 7162−7167.

(5) Ahmadi, M.; Wu, T.; Hu, B. A Review on Organic-Inorganic Halide Perovskite Photodetectors: Device Engineering and Fundamental Physics. *Adv. Mater.* **2017**, *29* (41), 1605242.

(6) Stranks, S. D.; Burlakov, V. M.; Leijtens, T.; Ball, J. M.; Goriely, A.; Snaith, H. J. Recombination Kinetics in Organic-Inorganic Perovskites: Excitons, Free Charge, and Subgap States. *Phys. Rev. Appl.* **2014**, *2* (3), 34007.

(7) Dou, L.; Yang, Y.; You, J.; Hong, Z.; Chang, W.-H.; Li, G.; Yang, Y. Solution-Processed Hybrid Perovskite Photodetectors with High Detectivity. *Nat. Commun.* **2014**, *5* (1), 5404.

(8) Hu, X.; Zhang, X.; Liang, L.; Bao, J.; Li, S.; Yang, W.; Xie, Y. High-Performance Flexible Broadband Photodetector Based on Organolead Halide Perovskite. *Adv. Funct. Mater.* **2014**, *24* (46), 7373−7380.

(9) Zhou, J.; Huang, J. S. Photodetectors Based on Organic-Inorganic Hybrid Lead Halide Perovskites. *Adv. Sci.* **2018**, *5* (1), 1700256.

(10) Dong, Y.; Gu, Y.; Zou, Y.; Song, J.; Xu, L.; Li, J.; Xue, J.; Li, X.; Zeng, H. Improving All-Inorganic Perovskite Photodetectors by Preferred Orientation and Plasmonic Effect. *Small* **2016**, *12* (40), 5622−5632.

(11) Li, D.; Dong, G.; Li, W.; Wang, L. High Performance Organic-Inorganic Perovskite-Optocoupler Based on Low-Voltage and Fast Response Perovskite Compound Photodetector. *Sci. Rep.* **2015**, *5* (1), 7902.

(12) Yu, G.; Pakbaz, K.; Heeger, A. J. Optocoupler Made from Semiconducting Polymers. *J. Electron. Mater.* **1994**, *23* (9), 925−928.

(13) Dong, G.; Zheng, H.; Duan, L.; Wang, L.; Qiu, Y. High-Performance Organic Optocouplers Based on a Photosensitive Interfacial C_{60}/NPB Heterojunction. *Adv. Mater.* **2009**, *21* (24), 2501−2504.

(14) Wang, Z.; Deng, J.; Wu, X.; Jing, N.; Hu, Z.; Cheng, X.; Hua, Y.; Wei, J.; Yin, S. The Relationship of Current Transfer Ratio and

Input Light Wavelengths in the Organic Photocoupler. *Appl. Phys. Lett.* **2009**, *94* (19), 193303.
(15) Dong, G.; Hu, Y.; Jiang, C.; Wang, L.; Qiu, Y. Organic Photocouplers Consisting of Organic Light-Emitting Diodes and Organic Photoresistors. *Appl. Phys. Lett.* **2006**, *88* (5), 051110.
(16) Yao, Y.; Chen, H. Y.; Huang, J.; Yang, Y. Low Voltage and Fast Speed All-Polymeric Optocouplers. *Appl. Phys. Lett.* **2007**, *90* (5), 053509.
(17) Yao, J. S.; Ge, J.; Han, B. N.; Wang, K. H.; Yao, H. B.; Yu, H. L.; Li, J. H.; Zhu, B. S.; Song, J. Z.; Chen, C.; Zhang, Q.; Zeng, H. B.; Luo, Y.; Yu, S. H. Ce^{3+}-Doping to Modulate Photoluminescence Kinetics for Efficient $CsPbBr_3$ Nanocrystals Based Light-Emitting Diodes. *J. Am. Chem. Soc.* **2018**, *140* (10), 3626−3634.
(18) Liang, F. X.; Wang, J. Z.; Zhang, Z. X.; Wang, Y. Y.; Gao, Y.; Luo, L. B. Broadband, Ultrafast, Self-Driven Photodetector Based on Cs-Doped $FAPbI_3$ Perovskite Thin Film. *Adv. Opt. Mater.* **2017**, *5* (22), 1700654.
(19) Li, Z.; Yang, M.; Park, J. S.; Wei, S. H.; Berry, J. J.; Zhu, K. Stabilizing Perovskite Structures by Tuning Tolerance Factor: Formation of Formamidinium and Cesium Lead Iodide Solid-State Alloys. *Chem. Mater.* **2016**, *28* (1), 284−292.
(20) Fu, Q. X.; Tang, X. L.; Huang, B.; Hu, T.; Tan, L. C.; Chen, L.; Chen, Y. W. Recent Progress on the Long-Term Stability of Perovskite Solar Cells. *Adv. Sci.* **2018**, *5* (5), 1700387.
(21) Zheng, X.; Wu, C.; Jha, S. K.; Li, Z.; Zhu, K.; Priya, S. Improved Phase Stability of Formamidinium Lead Triiodide Perovskite by Strain Relaxation. *ACS Energy Lett.* **2016**, *1* (5), 1014−1020.
(22) Zhang, L.; Yang, X.; Jiang, Q.; Wang, P.; Yin, Z.; Zhang, X.; Tan, H.; Yang, Y. M.; Wei, M.; Sutherland, B. R.; Sargent, E. H.; You, J. B. Ultra-Bright and Highly Efficient Inorganic Based Perovskite Light-Emitting Diodes. *Nat. Commun.* **2017**, *8*, 15640.
(23) Zhang, X.; Xu, B.; Wang, W.; Liu, S.; Zheng, Y.; Chen, S.; Wang, K.; Sun, X. W. Plasmonic Perovskite Light-Emitting Diodes Based on the Ag−$CsPbBr_3$ System. *ACS Appl. Mater. Interfaces* **2017**, *9* (5), 4926−4931.
(24) Li, J.; Xu, L.; Wang, T.; Song, J.; Chen, J.; Xue, J.; Dong, Y.; Cai, B.; Shan, Q.; Han, B. N.; Zeng, H. B. 50-Fold EQE Improvement up to 6.27% of Solution-Processed All-Inorganic Perovskite $CsPbBr_3$ QLEDs via Surface Ligand Density Control. *Adv. Mater.* **2017**, *29* (5), 1603885.
(25) Fang, Y.; Huang, J. Resolving Weak Light of Sub-Picowatt per Square Centimeter by Hybrid Perovskite Photodetectors Enabled by Noise Reduction. *Adv. Mater.* **2015**, *27* (17), 2804−2810.
(26) Kruangam, D.; Wongwan, F.; Chutarasok, T.; Chirakawikul, K.; Panyakeow, S. Amorphous Photocoupler Consisting of a-SiC : H Thin Film Light Emitting Diode and a-SiGe : H Thin Film Photodiode. *J. Non-Cryst. Solids* **2000**, *269* (99), 1241−1246.
(27) Zhang, X. L.; Xu, B.; Zhang, J. B.; Gao, Y.; Zheng, Y. J.; Wang, K.; Sun, X. W. All-Inorganic Perovskite Nanocrystals for High-Efficiency Light Emitting Diodes: Dual-Phase $CsPbBr_3$-$CsPb_2Br_5$ Composites. *Adv. Funct. Mater.* **2016**, *26* (25), 4595−4600.
(28) Lang, F.; Nickel, N. H.; Bundesmann, J.; Seidel, S.; Denker, A.; Albrecht, S.; Brus, V. V.; Rappich, J.; Rech, B.; Landi, G.; Neitzert, H. Radiation Hardness and Self-Healing of Perovskite Solar Cells. *Adv. Mater.* **2016**, *28* (39), 8726−8731.
(29) Veldhuis, S. A.; Ng, Y. F.; Ahmad, R.; Bruno, A.; Jamaludin, N. F.; Damodaran, B.; Mathews, N.; Mhaisalkar, S. G. Crown Ethers Enable Room-Temperature Synthesis of $CsPbBr_3$ Quantum Dots for Light-Emitting Diodes. *ACS Energy Lett.* **2018**, *3* (3), 526−531.
(30) Grubor, J.; Randel, S.; Langer, K. D.; Walewski, J. W. Broadband Information Broadcasting Using LED-Based Interior Lighting. *J. Lightwave Technol.* **2008**, *26* (24), 3883−3892.

DOI: 10.1021/acsami.8b15213
ACS Appl. Mater. Interfaces 2018, 10, 39441−39447